Complex harmonic wave scattering as the framework for investigation of bounded beam reflection and transmission at plane interfaces and its importance in the study of vibrational modes

K. Van Den Abeele[a] and O. Leroy
Interdisciplinary Research Center, K.U.L. Campus Kortrijk, B-8500 Kortrijk, Belgium

(Received 6 January 1992; accepted for publication 24 September 1992)

Deformation of bounded beams, when reflected from or transmitted through layered media, have always been discussed in connection with the generation of surface waves assuming an inhomogeneous field of leaking energy reradiating from the interface and interfering with the reflected or transmitted wave. By extending the theory of Claeys and Leroy [J. Acoust. Soc. Am. **72**, 585–590 (1982)], who introduced a description of a bounded beam by means of inhomogeneous waves, it is possible to separate the scattered profile from the leaky wave component and prove that all of the features occurring in the neighborhood of critical angles can be explained as purely reflection/transmission phenomena of particular complex harmonic waves, where no propagation along the interface or reradiation is involved. The findings are illustrated for various profiles incident on different layered media both for reflection and for transmission.

PACS numbers: 43.35.Pt, 43.35.Mr, 43.20.Gp

INTRODUCTION

When homogeneous plane waves reflect with mode conversion from or refract through an interface between two viscoelastic media, inhomogeneous plane waves are generated with exponentially decaying amplitudes along the wave fronts.[1–3] Such waves can be called complex harmonic waves, because of their complex-valued wave vectors, or alternatively also heterogeneous waves. Although most interest has always been shown for classical plane homogeneous waves, heterogeneous waves are the most general solution of the wave equation for a homogeneous and isotropic linearly viscoelastic material. Futhermore, surface waves cannot be described by homogeneous waves but it is well known that they are locally a combination of heterogeneous waves.[4] A thorough investigation of these waves in acoustics has started only recently.[5–9] Reflection and transmission properties for heterogeneous waves at layered media are found to be highly dependent upon the physical makeup of the sample under consideration. The nature of Rayleigh, Stoneley, and Lamb waves are related to poles of the reflection coefficients occurring at specific heterogeneity angle of incidence combinations.[10] Claeys and Leroy[11] were the first to use bulk heterogeneous waves as fundamental parts of the description of a bounded beam. Their theory predicted the same profile deformations as was found with Fourier analysis. However, the restriction in the decomposition of the incident bounded beam to complex harmonic waves with positive heterogeneity (decaying towards the upper surface of the layered medium) prohibited them from explicitly showing the presence of interface waves.

In the present paper we will interpret bounded beam deformations at layered media with plane interfaces in terms of the reflection and transmission coefficients for bulk heterogeneous waves, with both positive and negative heterogeneity, and prove the existence of surface waves as part of the scattered field. In contrast with the classical ray formalism explaining the generation of surface waves as a temporary conversion of a homogeneous wave into a surface wave that propagates over a certain distance along the interface and then reradiates by conversion into a heterogeneous bulk wave, no propagation nor reradiation is involved in our model. Apart from a meaningful physical interpretation, other advantages of the heterogeneous wave decomposition of bounded beams are the ability to describe nonspecular effects at large angles of incidence and the prediction of an optimum beamwidth range in order to generate strong surface waves and to observe large deformations in their profiles. We will verify these statements with a large number of illustrations.

I. COMPLEX HARMONIC WAVE REFLECTION AND TRANSMISSION

A. Representation of a complex harmonic wave in a viscoelastic medium

Following the pioneering work performed in electromagnetism and optics, the complex harmonic acoustic wave, propagating in an infinite isotropic, homogeneous, isotherm but viscoelastic medium with constant acoustic characteristics and initially at rest, has been described in detail by many specialists in acoustics.[1–9] The geometry is shown in Fig. 1.

Taking into account only "in plane" motions (no shear-

[a] Aspirant of the Belgian National Foundation for Scientific Research.

 0001-4966/93/010308-16$00.80

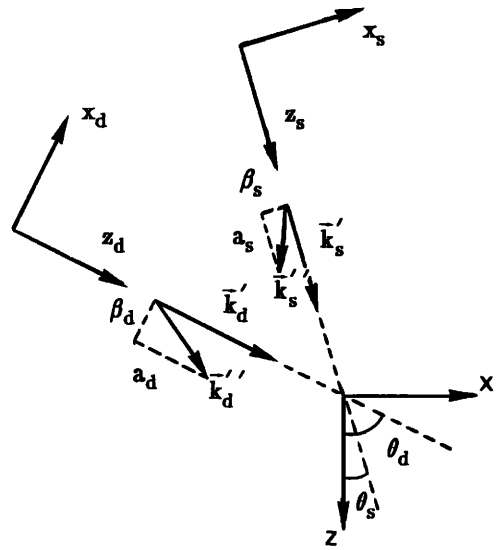

FIG. 1. Vector representation of heterogeneous waves.

horizontal waves), the general mathematical representation of x and z displacements of such waves in a solid medium can be expressed in terms of potential functions $\phi(x,z,t)$ and $\psi(x,z,t)$, which both satisfy a Helmholtz equation

$$\begin{aligned}\phi(x,z,t) &= \tilde{\phi}(x,z)e^{-i\omega t}, \quad [\Delta_{xz} + \kappa_d^2]\tilde{\phi}(x,z) = 0,\\ \psi(x,z,t) &= \tilde{\psi}(x,z)e^{-i\omega t}, \quad [\Delta_{xz} + \kappa_s^2]\tilde{\psi}(x,z) = 0,\end{aligned} \tag{1}$$

where Δ_{xz} is the Laplace operator $\partial^2/\partial x^2 + \partial^2/\partial z^2$, ω is the circular frequency, t is the time, and κ_d and κ_s are the complex-valued wave numbers for the dilatational and shear wave components. These potential functions ϕ and ψ may be written as

$$\begin{aligned}\phi(x,z,t) &= A_d \exp[i(\mathbf{k}_d\cdot\mathbf{r} - \omega t)],\\ \psi(x,z,t) &= A_s \exp[i(\mathbf{k}_s\cdot\mathbf{r} - \omega t)],\end{aligned} \tag{2a}$$

and are solutions of Eq. (1) provided that

$$\mathbf{k}_d\cdot\mathbf{k}_d = \kappa_d^2 \quad \text{and} \quad \mathbf{k}_s\cdot\mathbf{k}_s = \kappa_s^2. \tag{2b}$$

The displacements then follow from:

$$\begin{aligned}u_x(x,z,t) &= \left[\frac{\partial\phi}{\partial x} - \frac{\partial\psi}{\partial z}\right],\\ u_z(x,z,t) &= \left[\frac{\partial\phi}{\partial z} + \frac{\partial\psi}{\partial x}\right].\end{aligned} \tag{3}$$

In general A_d and A_s are complex constants while $\mathbf{k}_d$ and $\mathbf{k}_s$ are complex vectors. We will show the physical meaning of these vectors by considering for the moment only the dilatational component. Therefore we write $\mathbf{k}_d$ as $\mathbf{k}'_d + i\mathbf{k}''_d$, where the real-valued vector $\mathbf{k}'_d$ defines the angle θ_d with respect to the positive z direction, and $\mathbf{k}''_d$ (also real valued) can be decomposed into a component a_d along $\mathbf{k}'_d$ and a component β_d orthogonal to $\mathbf{k}'_d$ (Fig. 1). In terms of x_d–z_d coordinates we obtain the following more revealing expression for $\phi(x_d,z_d,t)$:

$$\begin{aligned}\phi(x_d,z_d,t) = A_d &\exp(\beta_d x_d)\exp(-a_d z_d)\\ &\times\exp[i(k'_d z_d - \omega t)],\end{aligned} \tag{4}$$

which is the mathematical description of a plane harmonic wave propagating in the z_d direction with a phase velocity ω/k'_d and—if β_d and a_d are both positive—decaying both in the negative x_d direction and in the positive z_d direction by different amounts: β_d represents the heterogeneity while a_d corresponds to the attenuation of the wave in the propagation direction. The planes z_d = constant are the planes of constant phase (wave fronts) and the planes $\beta_d x_d - a_d z_d$ = constant define the planes of constant amplitude.

With these definitions the x and z projections of the wave vector become:

$$\begin{aligned}[\mathbf{k}_d]_x &= [\mathbf{k}'_d]_x + i[\mathbf{k}''_d]_x\\ &= k'_d \sin\theta_d + ia_d \sin\theta_d - i\beta_d \cos\theta_d,\\ [\mathbf{k}_d]_z &= [\mathbf{k}'_d]_z + i[\mathbf{k}''_d]_z\\ &= k'_d \cos\theta_d + ia_d \cos\theta_d + i\beta_d \sin\theta_d,\end{aligned} \tag{5}$$

with

$$k'_d = |\mathbf{k}'_d|, \quad a_d = \frac{\mathbf{k}''_d\cdot\mathbf{k}'_d}{k'_d},$$

and

$$\beta_d = -\left[\mathbf{k}''_d - \frac{a_d\mathbf{k}'_d}{k'_d}\right]\cdot\mathbf{e}_{x_d}.$$

Depending on the values of β_d and a_d, the homogeneous ($\beta_d = 0, a_d = 0$), attenuated homogeneous ($\beta_d = 0$, $a_d \neq 0$), and pure inhomogeneous wave ($\beta_d \neq 0$, $a_d = 0$) can be derived. However, not all combinations of k'_d, a_d, and β_d are possible: Equation (2b), the complex dispersion relation, links the heterogeneous wave characteristics to two specific real-valued medium constants, v_d and α_d, respectively the acoustic velocity and attenuation. Written in terms of real quantities, this condition requires that

$$\begin{aligned}k'^2_d - a_d^2 - \beta_d^2 &= k_{0d}^2 - a_{0d}^2,\\ k'_d a_d &= k_{0d}\cdot a_{0d}\end{aligned} \tag{6}$$

with

$$k_{0d} = \omega/v_d, \quad a_{0d} = \omega^2\alpha_d, \quad \text{and} \quad k_{0d} + ia_{0d} = \kappa_d.$$

With only two equations for three unknowns, we may conclude that it is possible to obtain (in any medium in every direction and for each frquency) an infinite number of dilatational heterogeneous waves, characterized by the multiplet $(k_{0d},a_{0d},k'_d,a_d,\beta_d,\theta_d)$, where the first two constants specify the medium, the three following parameters determine the nature of the waves satisfying Eqs. (6), and θ_d defines the angle between the propagation direction and any fixed direction identified as the z axis of an orthogonal coordinate system. These interpretations and conclusions also hold for the case of shear waves in a solid medium.

B. Reflection and transmission of heterogeneous waves

We assume that a heterogeneous wave characterized by k'_m, a_m, β_m ($m = d$ or s), satisfying the dispersion relations, is incident at an angle θ_m on a plane interface between two viscous media. In general this wave will split its energy

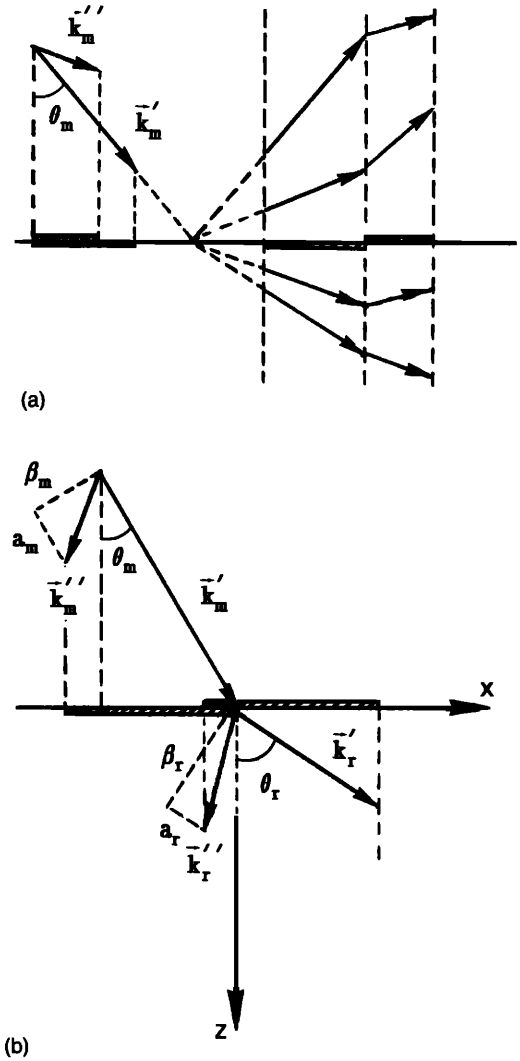

FIG. 2. (a) Complex harmonic wave scattering at a plane boundary between two solids. (b) Geometrical representation of the generalized Snell–Descartes laws.

into two reflected (one dilatational and one shear) and two transmitted (one dilatational and one shear) heterogeneous waves [Fig. 2(a)] with different directions. The nature of these waves and their directions with respect to the z axis follow immediately from the fact that continuity is required at the boundary of both media in combination with the complex dispersion relations for the new propagation medium.[12–17]

The continuity conditions demand invariability of the x coordinate, leading to the generalized Snell–Descartes laws [Fig. 2(b)]:

$$k'_r \sin\theta_r = k'_m \sin\theta_m,$$
$$a_r \sin\theta_r - \beta_r \cos\theta_r = a_m \sin\theta_m - \beta_m \cos\theta_m, \tag{7a}$$

where the subscript r refers to any of the four generated waves. In addition the new dispersion relations have to be satisfied:

$$k'^2_r - a^2_r - \beta^2_r = k^2_{0r} - a^2_{0r},$$
$$k'_r \cdot a_r = k_{0r} \cdot a_{0r}. \tag{7b}$$

As k_{0r} and a_{0r} are known medium constants (for a given frequency) Eqs. (7a) and (7b) form a set of four real (nonlinear) equations in four unknown variables: k'_r, a_r, β_r, and θ_r. Techniques to solve this set are described for several cases by Deschamps *et al.*[13] In order to deal with reflection, one can always first treat the generated reflected wave as being transmitted through an imaginary interface between two identical media, followed by mirroring the resulting wave with respect to the interface: $(k_{0r},a_{0r},k'_r,a_r,\beta_r,\theta_r) \rightarrow (k_{0r},a_{0r},k'_r,a_r,-\beta_r,\pi-\theta_r)$.

As important results and curiosities, we recall that homogeneous waves can generate inhomogeneous bulk waves if at least one of the two media is absorptive; inhomogeneous waves can generate homogeneous waves; under certain circumstances angles of refraction θ_r larger than 90° can be obtained and even a sequence of diminishing refraction angles for growing incident angles θ_m. Also, the fact that the same complex harmonic wave incident at θ_m and at $-\theta_m$ generate a different set of heterogeneous waves is quite remarkable. Furthermore, if the multiplet $(k_{0m}, a_{0m},k'_i,a_m,\beta_m,\theta_m)$ leads to the solution $(k_{0r},a_{0r},k'_r,a_r, \beta_r,\theta_r)$, it is not generally the case that $(k_{0m},a_{0m}, k'_i,a_m,-\beta_m,\theta_m)$ brings up the solution $(k_{0r},a_{0r},k'_r, a_r,-\beta_r,\theta_r)$ as one would expect. This will have important consequences in the study of the reflection and transmission through a layered medium.

The determination of reflection and transmission coefficients for the scattering of a plane acoustic wave incident on a layered medium has been described in detail by Brekhovskikh[18] for homogeneous waves and nonabsorbing layers. In order to include attenuation and heterogeneity, it is advisable to work from the beginning with complex valued quantities such as the different dilatational and shear wave numbers rather than real-valued velocities and to avoid expressions as functions of real angles ($\sin\theta$,$\cos\theta$,...) but preferably use the complex valued x and z wave-vector projec-

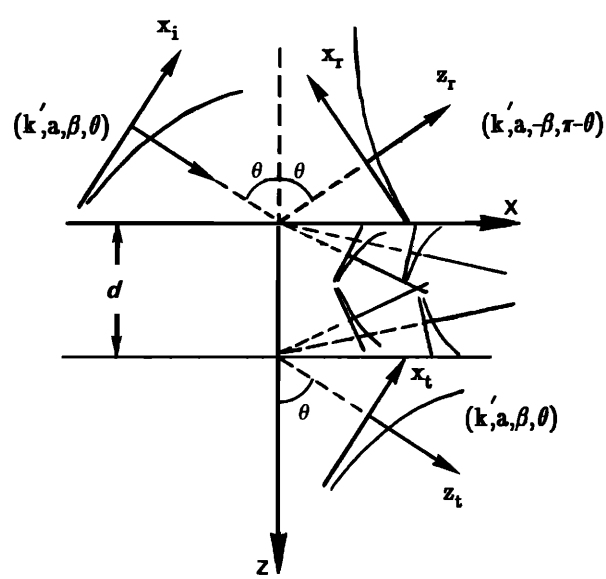

FIG. 3. Complex harmonic wave scattering at a solid layer immersed in water.

tions. Brekhovskikh's formulation, however, can be followed step by step without any changes.

In the present study, we will restrict ourselves to the case of a solid plate of thickness d immersed in a liquid bath. As a consequence only dilatational waves can insonify the plate, and only this type of wave has to be considered in reflection and transmission. Therefore we can omit the subscript of the incident, reflected, and transmitted wave without confusion.

We assume that a longitudinal heterogeneous wave with multiplet $(k_{0\text{liq}}, a_{0\text{liq}}, k', a, \beta, \theta)$ and $k_x = k' \sin\theta + ia \sin\theta - i\beta \cos\theta$ is incident on the solid layer at an angle θ and generates a reflected and transmitted longitudinal wave in the liquid, and up and downwards traveling dilatational and shear waves in the solid (Fig. 3). The angle, phase velocity, attenuation, and heterogeneity characteristic for each generated wave can be calculated by solving the nonlinear set of equations (7) considering appropriate medium constants.

Brekhovskikh's theory, applied for complex wave numbers, then yields the following expressions for the complex-valued reflected and transmitted amplitudes:

$$R(k_x) = \frac{RN(k_x)}{F_s(k_x)\cdot F_a(k_x)}, \tag{8}$$

$$T(k_x) = \frac{TN(k_x)}{F_s(k_x)\cdot F_a(k_x)}, \tag{9}$$

with

$$RN(k_x) = (\kappa_s^2 - 2k_x^2)^4 + 16k_x^4\zeta_d^2\zeta_s^2 - \rho^2\kappa_s^8\zeta_d^2/\zeta^2 + 8k_x^2\zeta_d\zeta_s(\kappa_s^2 - 2k_x^2)^2 \times [1 - \cos(d\zeta_d)\cos(d\zeta_s)] \times [\sin(d\zeta_d)\sin(d\zeta_s)]^{-1},$$

$$TN(k_x) = 2i\rho\kappa_s^4\zeta_d/\zeta\,[(\kappa_s^2 - 2k_x^2)^2/\sin(d\zeta_d) + 4k_x^2\zeta_d\zeta_s/\sin(d\zeta_s)],$$

$$F_s(k_x) = (\kappa_s^2 - 2k_x^2)^2\cot(d\zeta_d/2) + 4k_x^2\zeta_d\zeta_s\cot(d\zeta_s/2) - i\rho\kappa_s^4\zeta_d/\zeta,$$

$$F_a(k_x) = (\kappa_s^2 - 2k_x^2)^2\tan(d\zeta_d/2) + 4k_x^2\zeta_d\zeta_s\tan(d\zeta_s/2) + i\rho\kappa_s^4\zeta_d/\zeta.$$

Here, κ, κ_d, κ_s are the complex valued wave-number constants (for a specific frequency) inherent to longitudinal waves in the liquid and dilatational and shear waves in the solid, ρ is the ratio of liquid to solid mass densities, and $\zeta^2 = \kappa^2 - k_x^2$, $\zeta_d^2 = \kappa_d^2 - k_x^2$, and $\zeta_s^2 = \kappa_s^2 - k_x^2$.

Some examples illustrating the behavior of the modulus of reflection and transmission coefficients as function of angle of incidence and heterogeneity are shown in Fig. 4 (brass plate, $fd = 2.5$) and Fig. 5 (stainless steel plate, $fd = 4.0$). The medium constants used in the calculations are listed in Table I.

As carefully examined in Refs. 19–21, the roots of the denominator of R and T correspond to the x components of the wave numbers of the leaky Lamb modes:

for the symmetrical Lamb modes $F_s(k_x) = 0$,
for the asymmetrical Lamb modes $F_a(k_x) = 0$.

If k_x^L is such a root, one can easily find the exact Lamb angle, phase velocity, attenuation, and heterogeneity of the corresponding leaky Lamb wave components in the liquid at both sides of the plate by solving:

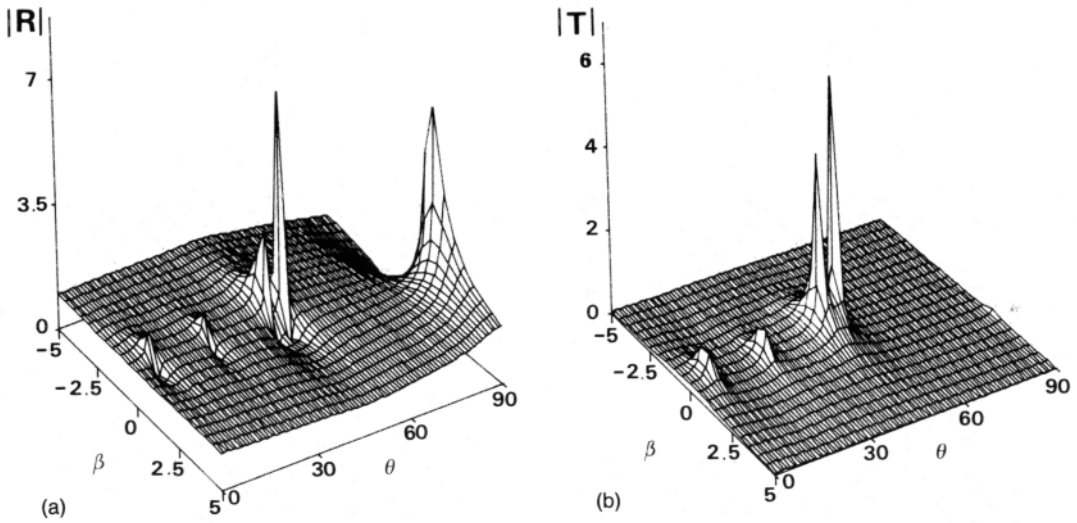

FIG. 4. Heterogeneous wave reflection (4a) and transmission coefficients (4b) as a function of angle of incidence and heterogeneity for a viscous brass plate of thickness 0.5 mm in water at 5-MHz frequency. Peaks correspond to S_2, A_1, S_0, and A_0 Lamb modes and to the Stoneley mode. The S_1 mode at an angle of about 19.6° ($\approx\theta_{1c}$) is not noticeable with the actual grid.

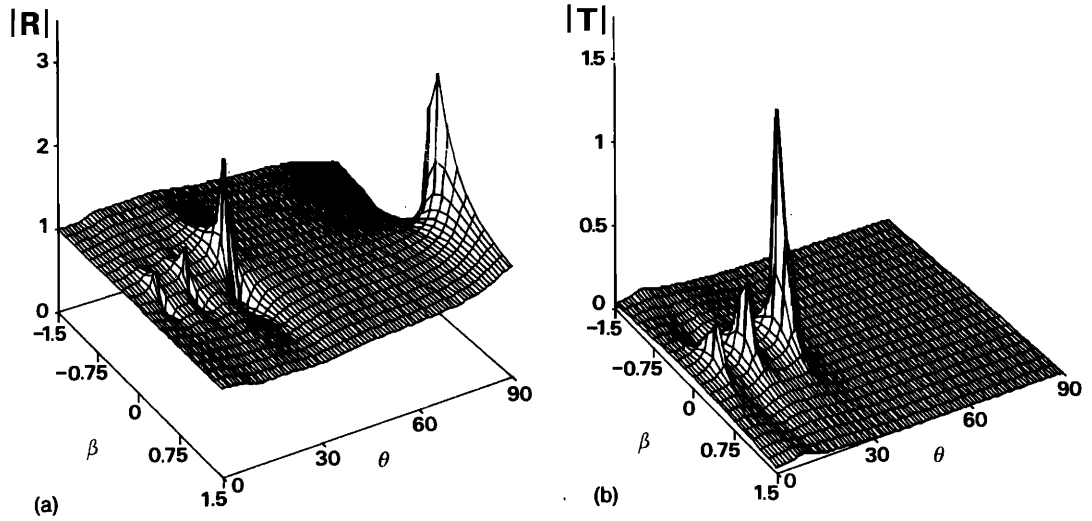

FIG. 5. Heterogeneous wave reflection (5a) and transmission coefficients (5b) as a function of angle of incidence and heterogeneity for a viscous stainless steel plate of thickness 2.0 mm in water at 2-MHz frequency.

$$k_L \sin\theta_L = \mathrm{Re}(k_x^L),$$
$$a_L \sin\theta_L - \beta_L \cos\theta_L = \mathrm{Im}(k_x^L),$$
$$k_L^2 - a_L^2 - \beta_L^2 = k_{0\mathrm{liq}}^2 - a_{0\mathrm{liq}}^2,$$
$$k_L \cdot a_L = k_{0\mathrm{liq}} \cdot a_{0\mathrm{liq}}. \quad (10)$$

Note that, as β_L is usually not equal to zero, there is a slight difference between k_L and $k_{0\mathrm{liq}}$. Therefore, the exact Lamb angle is somewhat different from the one found in the literature,[19–21] which is usually incorrectly defined by

$$\sin\theta_L = \mathrm{Re}(k_x^L)/k_{0\mathrm{liq}}.$$

The solution $(k_L, a_L, \beta_L, \theta_L)$ with $0 \leqslant \theta_L < \pi/2$ has to be interpreted as the particular incident complex harmonic wave for which leaky Lamb waves are generated traveling inside the plate with velocity $\omega/\mathrm{Re}(k_x^L)$ along the x direction, while energy is leaking through the interfaces above and underneath the plate [Fig. 6(a)]. These energy flows are represented by two heterogeneous wave: $(k_L, a_L, -\beta_L, \pi - \theta_L)$ in reflection and $(k_L, a_L, \beta_L, \theta_L)$ in transmission.[4] Furthermore, the expression for the reflected potential function along the interface $(z = 0)$ in the liquid corresponds to

$$R(k_x)\exp(\beta_L x \cos\theta_L)\exp(-a_L x \sin\theta_L)$$
$$\times \exp[i(k_L x \sin\theta_L - \omega t)]. \quad (11)$$

TABLE I. Values of medium constants used in calculations.

	Dilatational velocity v_d [m/s]	Shear velocity v_s [m/s]	Dilatational attenuation $\alpha_d \times 10^{18}$ [s²/mm]	Shear attenuation $\alpha_s \times 10^{18}$ [s²/mm]	Density ρ [kg/m³]
Brass	4410	2150	30	130	8.6
Steel	5790	3200	50	150	7.9
Water	1480	···	0.6	···	1.0

This means that the amplitude of the particle displacements on the level of the interface is exponentially decaying (for $\beta_L < 0$) in the positive x direction. This interpretation will appear to be very useful when we discuss the trailing field of

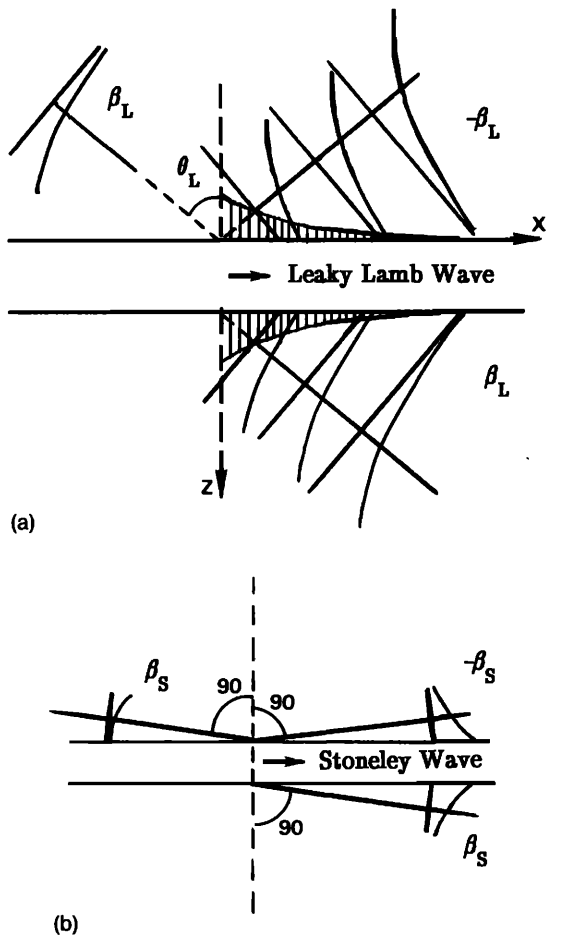

FIG. 6. (a) The leaky Lamb wave: a particular case of the reflection/transmission phenomena of complex harmonic waves. (b) The Stoneley wave: a resonance at 90°.

a bounded beam as a result of reflection/transmission. The characteristics of the waves inside the plate follow immediately from the generalized Snell–Descartes laws.

Close examination of Figs. 4 and 5 immediately yields all possible combinations (β,θ) that lead to the excitation of vibrational modes in the plate (peaks of R and T). Note however that due to the nonzero grid dimensions not all modes are visible on the three-dimensional figures. For the brass plate in Fig. 4, e.g., the peak corresponding to the Lamb mode located near the longitudinal critical angle is so sharp and small that we are not able to observe it with the grid used. However, its existence is beyond doubt, and could be shown by adjusting the grid spacing.

At grazing incidence we find another reflection surface mode: the Stoneley wave [Fig. 6(b)]. Substituting $\theta = 90°$ into Eq. (11), it is obvious that the amplitude of this wave remains constant while propagating, apart from a small reduction caused by attenuation in the liquid.

It is important to note that the excitation of surface waves has been explained here as a pure reflection/transmission phenomenon of heterogeneous waves. No temporary propagation along the surface and no re-emission was assumed. We will use this fact in the following section where we will build up a bounded beam by means of these types of waves.

II. BOUNDED BEAM REFLECTION AND TRANSMISSION:

A. Bounded beam representation

In most studies involving reflection and transmission of bounded beams, Fourier analysis is used in order to properly account for the bounded character of the ultrasonic beam before and after reflection/transmission.[21–26] This numerical integration technique uses an infinite spectrum of plane homogeneous waves with different directions to describe the beam profile. The resulting reflected and transmitted profiles clearly illustrate all of the attendant phenomena such as beam displacements, null-zones, and trailing field. We note, however, that it is not possible to prove the presence of a leaky Lamb wave component in the spectrum of the reflected or transmitted beam since homogeneous waves do not change their heterogeneity characteristics when reflected or transmitted in the same medium.

More recently Claeys and Leroy[11] introduced another method that accounts for the finite dimensions of an acoustic beam profile. Their method is based on the decomposition of a known profile into a finite discrete series of heterogeneous waves propagating in one specific direction. This concept also explains the nonspecular effects of deformation at critical angles.[27–29]

The fact that Fourier analysis is not straightforward on the matter of the generation of surface waves and that this method leads to numerical problems for small profiles and large angles, has stimulated us to investigate the method of Claeys and Leroy more thoroughly.

As we already mentioned earlier, the heterogeneous wave is the most general solution of the equation of motion. The problem being linear, any linear combination of heterogeneous waves satisfying the dispersion relations, will also be a solution of the wave equation, which means that general displacements can be expressed by a potential function of the following form:

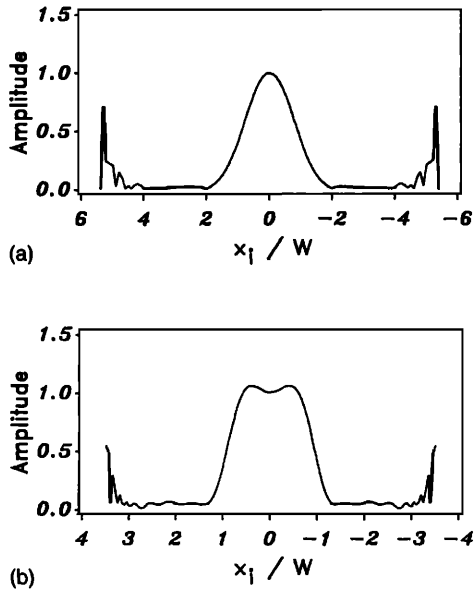

FIG. 7. Approximation of Gaussian and "square" profiles by means of a discrete series of heterogeneous waves with positive and negative heterogeneity coefficients.

$$\sum_{n=-\infty}^{+\infty} A_n e^{\beta_n x_i} e^{-a_n z_i} e^{i(k'_n z_i - \omega t)} \tag{12}$$

with for all values of the summation index n

$$k'^2_n - a_n^2 - \beta^2_n = k^2_{0\text{liq}} - a^2_{0liq},$$

$$k'_n \cdot a_n = k_{0\text{liq}} \cdot a_{0\text{liq}}$$

and

$$(k_x)_n = k'_n \sin\theta + ia_n \sin\theta - i\beta_n \cos\theta.$$

In their description of the incident profile, Claeys and Leroy restricted their analysis to inhomogeneous waves with amplitude variations along the wavefront that decay exponentially towards the upper side of the plate ($\beta_n \geqslant 0$). It is, however, a more general approach to use both decaying ($\beta_n \geqslant 0$) and exponentially growing ($\beta_n \leqslant 0$) heterogeneous waves. The advantage of this generalization will become clear in the present study.

Any profile defined by $f(x_i)$ at $z_i = 0$, can be approximated by a suitable combination of complex harmonic waves, such that their amplitude and heterogeneity satisfy

$$f(x_i) = \sum_{n=-\infty}^{+\infty} A_n e^{\beta_n x_i}. \tag{13}$$

Figure 7 illustrates the results for a Gaussian and a "square" profile using this method. Although divergence is an inherent and inevitable characteristic of the heterogeneous wave decomposition, we observe good approximation within several beamwidths.

Let us focus now on the reflection and transmission of a Gaussian beam of half-width W on a plate immersed in water. A fairly good approximation of this symmetrical profile was obtained by

TABLE II. Table of relative amplitudes A_n of the heterogeneous waves used in Eq. (14a) to build up a Gaussian profile (n,A_n).

0	−0.101585E00	8	−0.253160E02	16	−0.963892E-05	24	−0.116916E-15	32	−0.112837E-30
1	0.219627E01	9	0.801411E01	17	0.696972E-06	25	0.264569E-17	33	0.695937E-33
2	−0.209847E02	10	−0.202240E01	18	−0.432819E-07	26	−0.518114E-19	34	−0.347116E-35
3	0.775777E02	11	0.414019E00	19	0.231621E-08	27	0.875971E-21	35	0.136344E-37
4	−0.141464E03	12	−0.697106E-01	20	−0.107098E-09	28	−0.127424E-22	36	−0.405503E-40
5	0.155761E03	13	0.976173E-02	21	0.428722E-11	29	0.158749E-24	37	0.857345E-43
6	−0.115878E03	14	−0.114722E-02	22	−0.148771E-12	30	−0.168354E-26	38	−0.114701E-45
7	0.623143E02	15	0.114003E-03	23	0.447807E-14	31	0.150771E-28	39	0.729231E-49

$$\exp\left[-\left(\frac{x_i}{W}\right)^2\right] = \sum_{n=-39}^{+39} A_n e^{\beta_n x_i}, \tag{14a}$$

with

$$\beta_n = -\beta_{-n} = n/1.9W, \quad \text{for } n: -39\cdots 39, \tag{14b}$$

while the coefficients A_n ($=A_{-n}$) are given in Table II. An advantage of this method is that these coefficents are independent of the width of the profile so that they can be tabulated, which reduces the computing time.

B. Bounded beam reflection and transmission in terms of complex harmonic waves

Again, because of linearity, the amplitude and phase distribution of the reflected and transmitted field for any angle of incidence θ can be found by multiplying each heterogeneous wave by its complex valued reflection/transmission coefficient:

$$R(k'_n \sin\theta + ia_n \sin\theta - i\beta_n \cos\theta)$$

and

$$T(k'_n \sin\theta + ia_n \sin\theta - i\beta_n \cos\theta).$$

Under normal conditions, for reflection [where each multiplet $(k_{0\text{liq}},a_{0\text{liq}},k'_n,a_n,\beta_n,\theta)$ brings up the reflected complex harmonic wave $(k_{0\text{liq}},a_{0\text{liq}},k'_n,a_n,-\beta_n,\pi-\theta)$],

$$\sum_{n=-39}^{+39} R((k_x)_n)A_n e^{-\beta_n x_r} \tag{15}$$

will be a good approximation of the reflected profile at $z_r = 0$.

Suppose, however, that $(k_x)_n$ corresponds to a pole of the reflection coefficient (or close to a pole). In this case Eq. (15) will be influenced by the appearance of dominating heterogeneous waves and hence a smooth reflection profile cannot be obtained. Nevertheless, we found an important argument to deal with this nonconvergence, leading to a meaningful explanation of the physical phenomena occurring for these particular circumstances (Fig. 8). We will show that the reflected field [Eq. (15)] can be separated in two components with significant physical meaning.

Let us first assume that circumstances are such that $R(k_x)$ has a pole $(k_{x\text{pole}})$ with heterogeneity $\beta_{\text{pole}} < 0$ (which is the case for ordinary Lamb modes) and that the characteristics of the heterogeneous wave corresponding to this pole are close to those of one of the waves in the finite decomposition of the incident beam. Without affecting the energy balance, we can break apart the reflected field into two separate components, mathematically described by

$$R((k_x)_0)A_0 + 2\sum_{n=1}^{+39} R((k_x)_n)A_n e^{-\beta_n x_r} \tag{16a}$$

and

$$\sum_{n=-39}^{-1} R((k_x)_n)A_n e^{-\beta_n x_r} - \sum_{n=1}^{+39} R((k_x)_n)A_n e^{-\beta_n x_r} = \sum_{n=1}^{+39} A_n\left[R((k_x)_{-n})e^{\beta_n x_r} - R((k_x)_n)e^{-\beta_n x_r}\right], \tag{16b}$$

which interfere.

We will now show that the first component represents the reflected profile and that the second component can be associated with the presence of the leaky Lamb wave. Indeed, for reasons of symmetry, it is obvious that in the case of specular reflectivity $[R((k_x)_n) \approx 1 n: -39\cdots 39]$ Eq. (16a) describes the incident Gaussian profile again, while the expression (16b) converges to zero within the area of interest (no appearance of the leaky Lamb wave). On the other hand, when conditions are such that the decomposition of the incident beam [Eq. (14a)] contains complex harmonic waves with negative heterogeneity β_{-n} for which the reflection coefficient $R((k_x)_{-n})$ tends to a value much larger than one, the terms $R((k_x)_{-n})e^{\beta_n x_r}$ will dominate the additional part (16b) while the separation prohibits the diver-

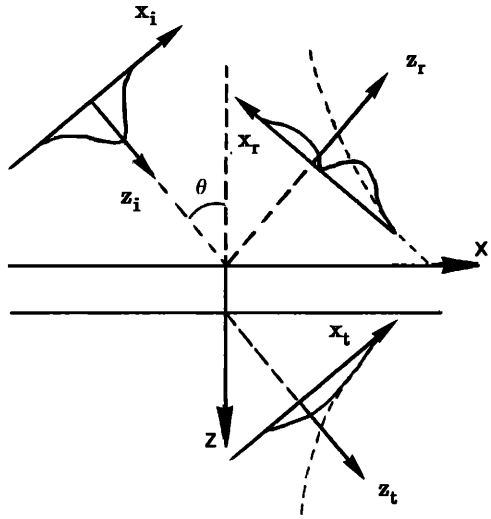

FIG. 8. Geometry of the reflection and transmission phenomena for bounded beams.

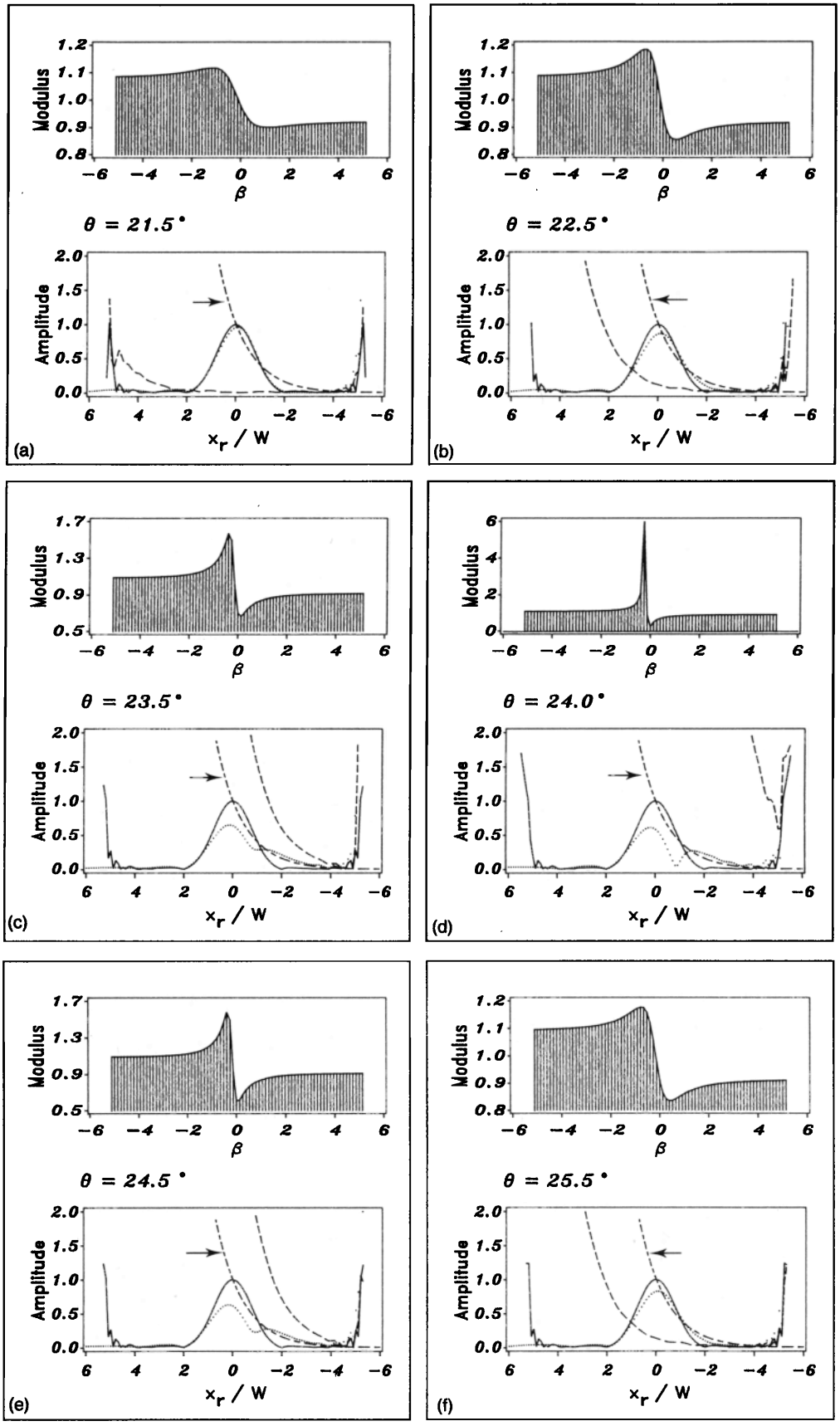

FIG. 9. Sequence of profile deformations in the reflected field of a Gaussian beam of 4-mm width, incident at angles in the neighborhood of a Lamb angle on a brass plate of 0.5 mm at 5 MHz. The incident profile is given by the full line. The two components in reflection, without interference, are represented by the dotted [formula (16a)] and the dashed line [formula (16b)]. As a reference, the dashed line marked with an arrow represents the nature of the exact leaky Lamb wave component (normalized) in the liquid. (a) $\theta = 21.5°$; (b) $\theta = 22.5°$; (c) $\theta = 23.5°$; (d) $\theta = 24°$; (e) $\theta = 24.5°$; (f) $\theta = 25.5°$. Above each profile illustration, the modulus of the reflection coefficient for the various heterogeneous waves is given as a function of their heterogeneity.

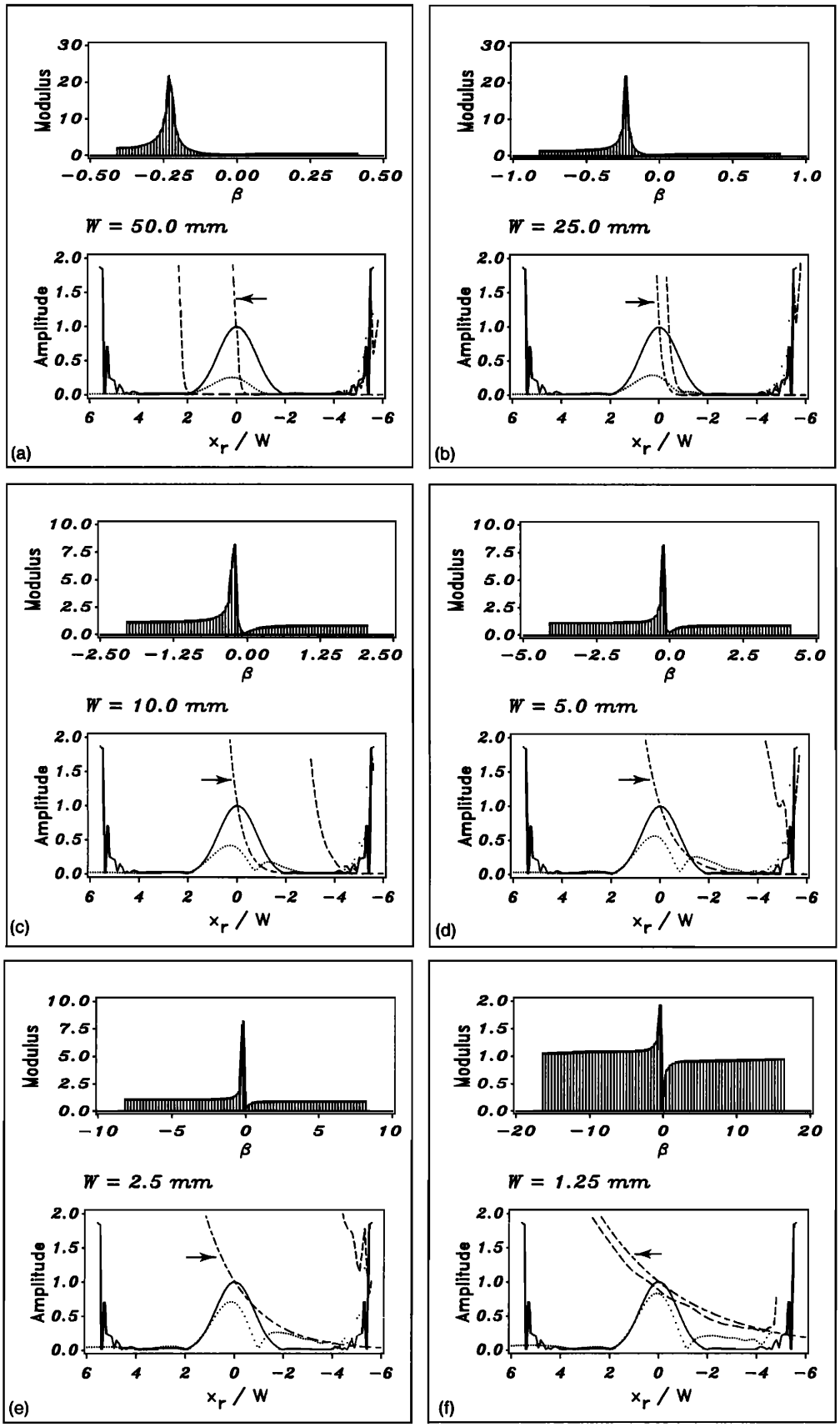

FIG. 10. Sequence of profile deformations in the reflected field of a Gaussian beam of variable width at Lamb angle incidence (24°) on a brass plate of 0.5 mm at 5 MHz. Incident profile: ——; attendant reflected profile [formula (16a)]: ····; surface wave component [formula (16b)]: ----. The dashed line marked with an arrow represents the exact nature of the leaky Lamb wave component. (a) $W = 50$ mm; (b) $W = 25$ mm; (c) $W = 10$ mm; (d) $W = 5$ mm; (e) $W = 2.5$ mm; (f) $W = 1.25$ mm.

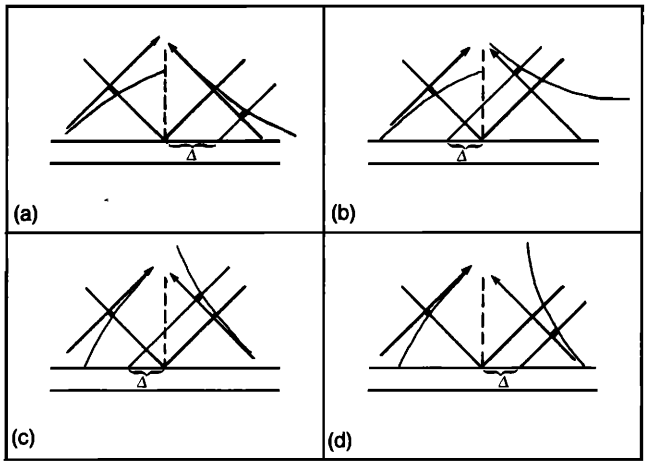

FIG. 11. Interpretation of the heterogeneous wave reflection coefficient in terms of geometrical displacement $\Delta \approx -\ln(|R|)/\beta\cos(\theta)$ along the interface. (a) $\beta>0\ |R|<1 \Rightarrow \Delta>0$; (b) $\beta>0\ |R|>1 \Rightarrow \Delta<0$; (c) $\beta<0\ |R|<1 \Rightarrow \Delta<0$; (d) $\beta<0\ |R|>1 \Rightarrow \Delta>0$.

gence of Eq. (16a) by having excluded them. Moreover, extensive calculations have shown that the field represented by Eq. (16a) corresponds almost exactly to what Fourier analysis predicts, with displacements, null zones, and other properties as expected. That is why we will speak about this first component as the attendant-reflected profile. The additional component [Eq. (16b)] contains the very important $A_n R((k_x)_{-n}) e^{\beta_n x_r}$ terms. If the coefficients A_n of the heterogeneous waves with the largest reflection coefficients are not too small, Eq. (16b) is dominated by these terms and its behavior is governed by a sum of exponentially growing functions with growing constants $-\beta_{-n}=\beta_n(>0)$, which are all very close to the decay characteristic of the leaky Lamb wave component generated in the fluid: $-\beta_{\text{pole}}$. The result is a function of which the path is similar to the curve of the exact Lamb wave (see Figs. 9 and 10). In other words, the presence of a leaky Lamb wave in the plate is connected to the contribution of the additional component (16b).

We illustrate this separation procedure in two sequences of figures: Figs. 9 and 10. Every illustration of profile deformation in the present study is accompanied by a figure, showing the variation of the reflection/transmission coefficient for the discrete heterogeneous waves that make up the incident profile. For both sequences, a Gaussian profile is assumed impinging with frequency 5 MHz upon a viscous brass plate of thickness 0.5 mm. The behavior of the heterogeneous wave reflection coefficient as a function of angle of incidence and heterogeneity for this case is given in Fig. 4. In Fig. 9, the reflection of a profile with constant incident width of 4 mm is investigated at different angles of incidence around 24°. Close to the Lamb angle, we expect the strongest nonspecular phenomena in the intensity distribution of the reflected field. Figure 9(d) shows that for this angle of incidence the component corresponding to the leaky Lamb wave field generated in the liquid [represented by the dashed line or Eq. (16b)] is at its maximum while the deformation of the reflected beam [dotted line or Eq. (16a)] is most pronounced. Moreover, in all subfigures we observe that the exponentially decaying behavior of the dashed line closely approximates the Lamb wave nature of the expected surface wave (dashed line marked with an arrow). The only difference between the various leaking energy components is a more or less pronounced shift to the right (direction of the plate). In connection with this remark, we must emphasize that the curve corresponding to Eq. (16b) in the nondiverging region on the x_r axis only represents a relative measurement of the importance of energy leaking into the liquid, and that the exponential behavior of its corresponding field only locally exists and locally interferes with the modified profile in the form of a decaying tail connecting the profile with the surface of the plate.[30] This means that instead of the infinite character of this component, we consider only the part that has physical meaning. The objection that the wave amplitude in the mathematical Lamb wave representation tends to infinity when traveling away from the surface is thereby refuted. Knowing what Schoch displacement means for infinite heterogeneous waves (Fig. 11), this tail can even be located far before the convergent part of the attendant reflected profile. A comparison of the x_r-coordinate values for which the amplitude of Eq. (16b) in the different cases is equal to unity provides essential information about the extent of this exponentially decaying trailing field.

Another sequence (Fig. 10) illustrates the influence of beamwidth variations on the leaky Lamb wave field at the Lamb angle of incidence $\theta_L = 24.0°$. The corresponding A_1 mode has a Lamb heterogeneity β_L approximately equal to -0.225/mm. We observe that once the beam is too wide, the peculiarities in the complex harmonic wave reflection coefficient are located too far from the region of incident heterogeneous waves with significant coefficients A_n, which results in not observing any leaking energy from a surface wave. Nevertheless, the profile is reduced in amplitude because of a global reflection coefficient smaller than unity for all heterogeneous waves in Eq. (16a). Reducing the beamwidth, the peculiarities shift toward smaller absolute values of the summation index n and therefore the exponential field becomes more and more noticeable. Since the most important coefficients in the decomposition of the incident beam are located between A_{-10} and A_{10}, it is obvious from Eq. (14b) that the optimum beamwidth in order to produce strong leaky Lamb wave reflection and large deformations at θ_L corresponds to a value smaller than $5.26/|\beta_L|$ [Fig. 10(c)–(f)].

The apparent change of the slope of the curves corresponding to the surface wave component in every subfigure of Fig. 10 is only due to the fact that the value x_r/W is plotted in abscissa. Although the curves become steeper for larger W, the decay coefficient remains the same in all subfigures (≈ 0.225/mm). One can take the amplitude value at $x_r = 0$ as a relative measurement of the importance of the surface wave component.

As we see in Figs. 4(a) and 5(a), one also must take into consideration the case of poles of the reflection coefficient for which $\beta_{\text{pole}} > 0$, e.g., at 90°, corresponding to the Stoneley wave. The procedure we follow for this case is essentially the same as for the first case with the modification that the

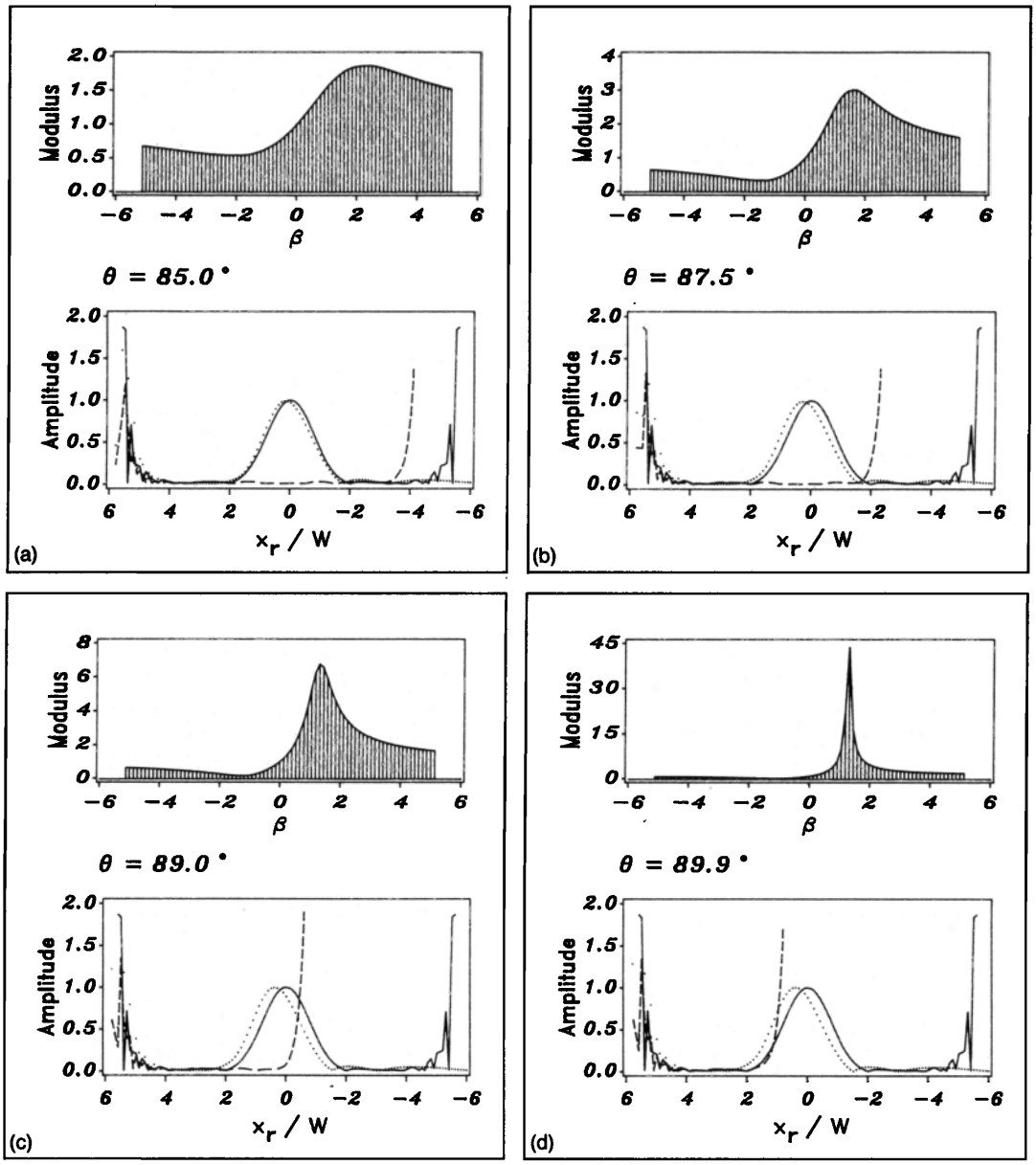

FIG. 12. Gaussian beam reflection (width = 4 mm) near grazing incidence on a brass plate of 0.5 mm at 5 MHz. Incident profile: ——; attendant reflected profile [formula (17a)]: ····; Stoneley wave component [formula (17b)]: ----. (a) $\theta = 85°$; (b) $\theta = 87.5°$; (c) $\theta = 89.0$; (d) $\theta = 89.9°$.

profile is now made up of

$$R((k_x)_0)A_0 + 2\sum_{n=1}^{+39} R((k_x)_{-n})A_{-n}e^{\beta_n x_r} \qquad (17a)$$

and the additional surface wave component in the liquid is given by

$$\sum_{n=1}^{+39} A_n\left[R((k_x)_n)e^{-\beta_n x_r} - R((k_x)_{-n})e^{\beta_n x_r}\right]. \qquad (17b)$$

If the amplitude decay corresponding to the inhomogeneous Stoneley wave is present is the sequence of heterogeneities involved in the decomposition of the incident profile, the reflected profile (17a) is displaced in the positive x_r direction, while the second component is governed by the Stoneley wave in the liquid itself (Fig. 12). We emphasize that it is far more difficult and nearly impossible to obtain these results when applying Fourier analysis.

Analogous separating procedures can be followed in the investigation of the transmitted field. Again, the total field can be separated into an attendant-transmitted profile that is essentially identical to the profile obtained by Fourier analysis, and an additional contribution representing the energy flow in the liquid beneath the plate due to generated leaky surface waves (Fig. 13). We note here that the nature and intensity of the Lamb wave radiation is the same in reflection as in transmission and that as a consequence the trailing field above and underneath the plate extends over comparable distances. This can also be observed in the experiments reported by Plona *et al.*[19,21]

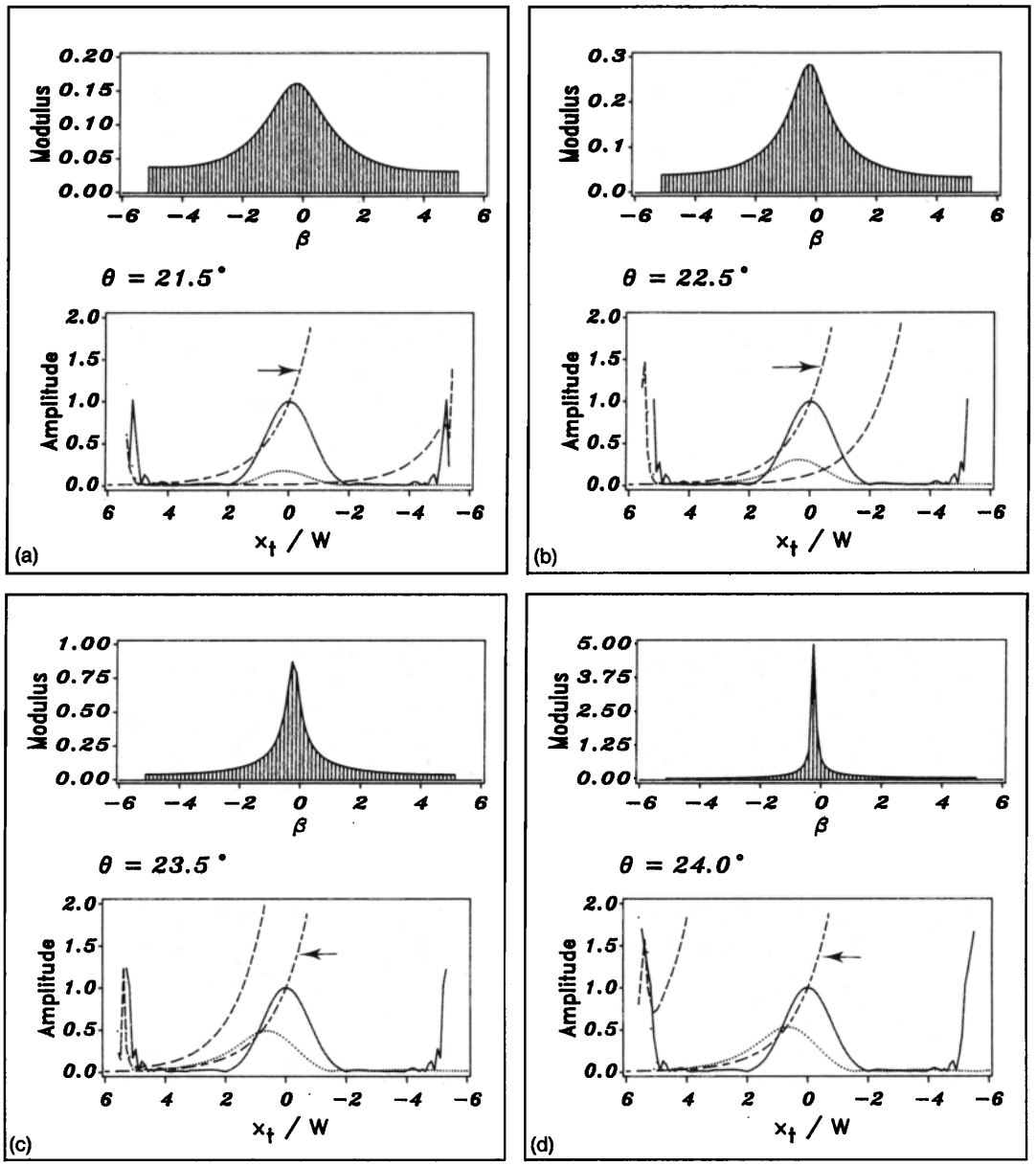

FIG. 13. Gaussian beam transmission (width = 4 mm) near Lamb angle (24°) through a brass plate of 0.5 mm at 5 MHz. Incident profile: ——; attendant transmitted profile [formula (16a)]: ···; surface wave component [formula (16b)]: ----. The dashed line marked with an arrow represents the exact nature of the leaky Lamb wave component. (a) $\theta = 21.5°$; (b) $\theta = 22.5$; (c) $\theta = 23.5°$; (d) $\theta = 24.0°$.

It is also possible to apply this separation procedure for other kinds of profiles, for instance the square profile which can be described as a combination of two overlapping Gaussian beams displaced in opposite direction over the same distance, or the side-lobe profile. Results for the square profile incident on a steel layer of thickness 2 mm at a frequency of 2 MHz are shown in Fig. 14.

Instead of investigating plates one can also examine any other kind of layered medium. Considering a halfspace as the limit of a thick plate (Fig. 15), the existence of the leaky Rayleigh mode component in the liquid can be demonstrated (Fig. 16).

Thin layers on substrates (or thick plates) hold the interest of many investigators. The three-dimensional plots in Fig. 17 represent the complex harmonic reflection moduli for different values of the thickness d of a steel layer mounted on a thick brass plate (at 5 MHz a brass plate of 2 mm is a reasonable approximation for a substrate). From a close look at this sequence, we can conclude that for values of the product frequency (f) times steel layer thickness (d) larger than a specific $(fd)_1$ the substrate remains invisible, while for values smaller than a certain $(fd)_2$ the layer cannot be observed anymore. Indeed, comparing Fig. 17(a) and (b) on the one side and Fig. 17(e) and (f) on the other side, we

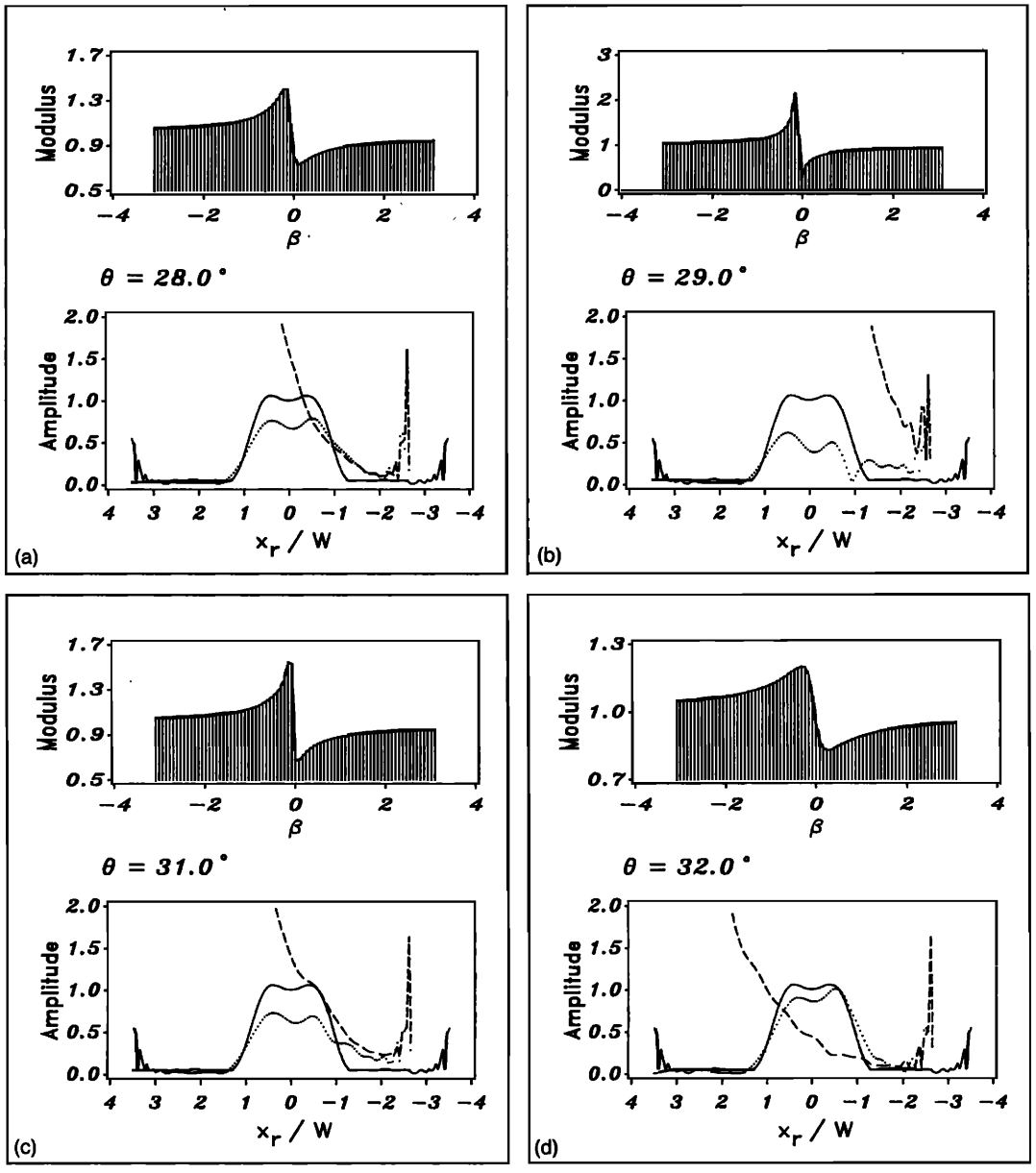

FIG. 14. "Square profile reflection (width = 4 mm) near Lamb angle (29°) through a stainless steel plate of 2.0 mm at 2 MHz. Incident profile: ——; attendant reflected profile: ····; leaky Lamb wave component: ----. (a) $\theta = 28°$; (b) $\theta = 29°$; (c) $\theta = 31°$; (d) $\theta = 32°$.

notice for large layer thicknesses only typical steel substrate phenomena and for small fd values mainly typical brass phenomena. The limit angle behind which no surface modes can be detected (except the Stoneley wave) moves from the Rayleigh angle for steel to the Rayleigh angle for brass, while the heterogeneity characteristic of the corresponding mode changes from the heterogeneity of a Rayleigh wave at a steel half-space to the heterogeneity of a Rayleigh wave at a brass substrate. Besides, at grazing incidence one observes a change in heterogeneity of the Stoneley waves from the specific heterogeneity of a Stoneley wave at a water–steel interface ($\beta_{sw} = 0.50$/mm and velocity $v = 1479.59$ m/s) to the heterogeneity of this type of surface waves at a water-brass boundary ($\beta_s = 1.287$/mm and velocity $v = 1477.29$ m/s). These two observations illustrate that both presence and nature of surface waves are extremely sensitive to thickness for investigation of thin films.

III. CONCLUSIONS

We have shown that the description of bounded beams by the method of Claeys and Leroy can be extended to a more general approximation using both positive and negative decaying heterogeneous waves. The total reflected and transmitted fields are found to be made up of an attendant profile and a leaky surface wave component exponentially decaying corresponding to the nature of the generated Ray-

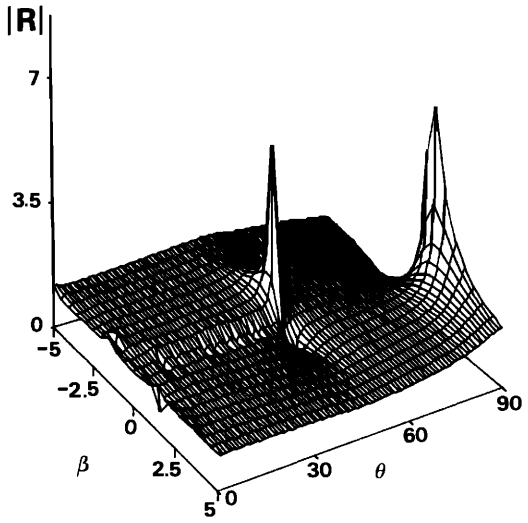

FIG. 15. Heterogeneous wave reflection coefficients as function of angle of incidence and heterogeneity for a "thick" viscous brass plate (3 mm) in water at 5-MHz frequency. The major peak at about 47.5° corresponds to the Rayleigh wave.

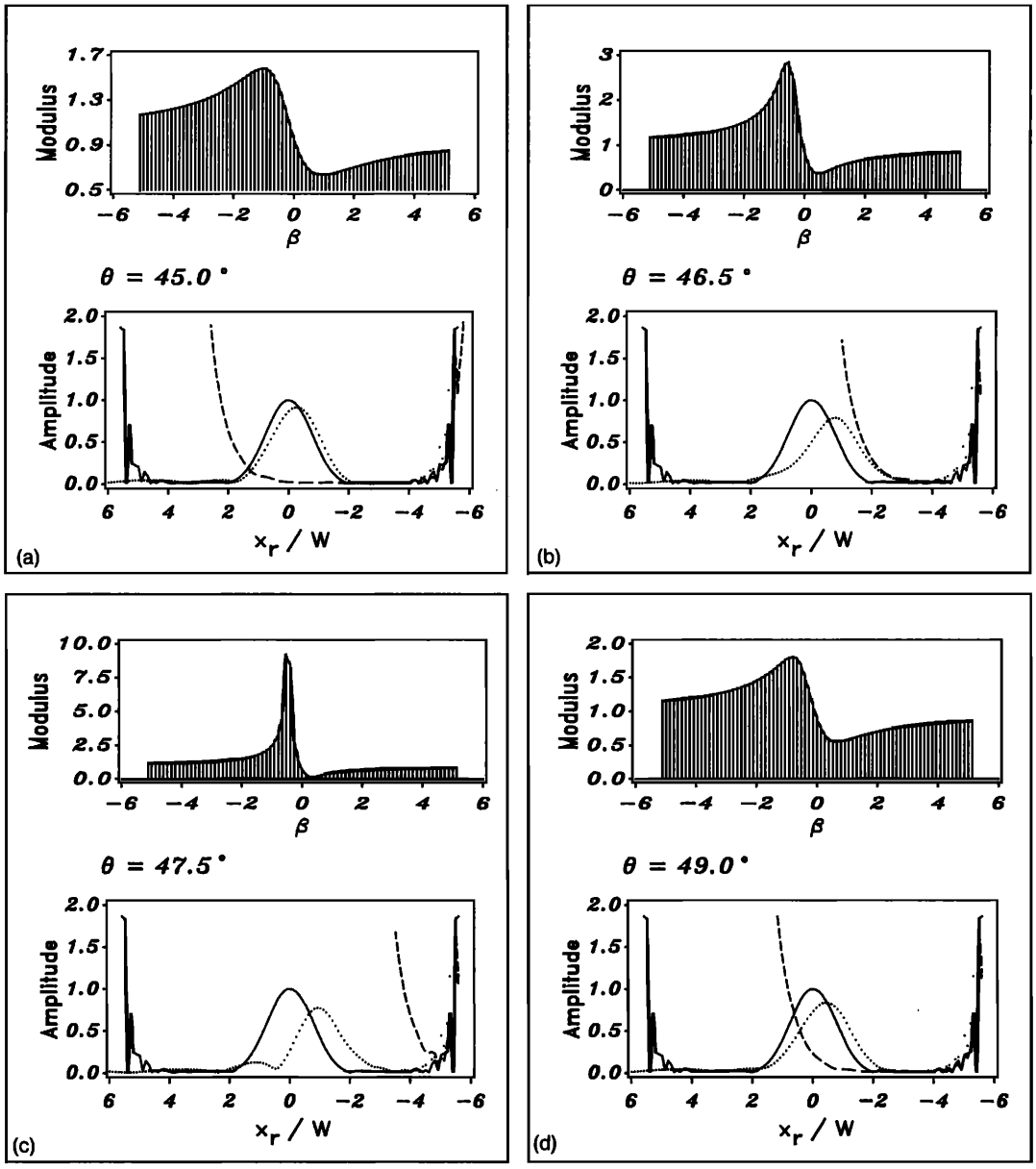

FIG. 16. Gaussian beam reflection (width = 4 mm) on a "thick" brass plate of 3 mm at 5 MHz near the Rayleigh angle. Incident profile: ——; attendant reflected profile: ····; Rayleigh wave component: ----; (a) $\theta = 45°$; (b) $\theta = 46.5°$; (c) $\theta = 47.5°$; (d) $\theta = 49.0°$.

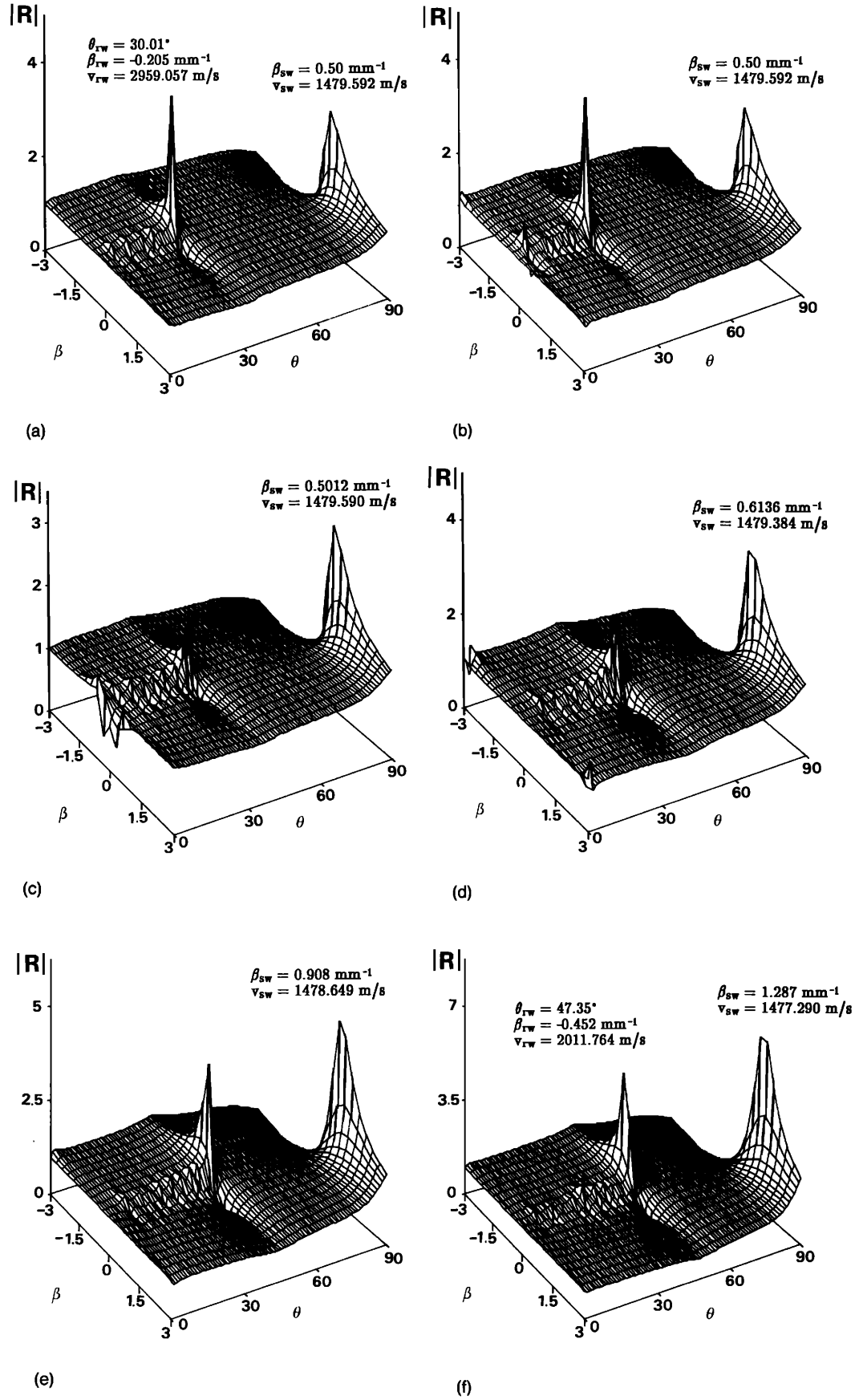

FIG. 17. Sequence of three-dimensional figures of the heterogeneous wave reflection coeffcients as function of angle of incidence and heterogeneity for different combinations of a steel–brass bilayer in water at 5 MHz. (a) 2-mm steel layer without brass plate; (b) 1-mm steel layer on a 2-mm-thick brass plate; (c) 0.25-Mm steel layer on a 2-mm-thick brass plate; (d) 0.1-mm steel layer on a 2-mm-thick brass plate; (e) 0.05-mm steel layer on a 2-mm-thick brass plate; (f) 2-mm-thick brass plate without steel layer.

leigh, Stoneley, or Lamb wave. However, the bulk inhomogeneous energy component can only be physically interpreted in a meaningful way as a local trailing field connecting the scattered profile to the surface of the reflector/transmitter under consideration. The important fact is that this phenomenon has been explained as a pure reflection/transmission effect in contrast with the classical approach of mode conversion of homogeneous waves into surface waves propagating along the interface and reradiating after a certain distance from the interface in the nature of a heterogeneous wave. The evidence of leaky wave components has been illustrated for various kinds of layered media, related to reflection and transmission and for different incident beam profiles.

[1]H. F. Cooper, Jr., "Reflection and Transmission of Oblique Plane Waves at a Plane Interface between Visco-elastic Media," J. Acoust. Soc. Am. **42**, 1064–1069 (1967).

[2]P. Kiełczyński and W. Pajewski, "Reflection of an Oblique Incident SH Plane Wave at a Plane Interface between an Elastic Solid and a Viscoelastic Liquid," J. Acoust. Soc. Am. **81**, 599–605 (1987).

[3]M. Deschamps and B. Hosten, "Génération de l'Onde Hétérogène de Volume dans un Liquide non Absorbant," Acustica **68**, 92–95 (1989).

[4]I. A. Viktorov, *Rayleigh and Lamb Waves: Physical Theory and Applications* (Plenum, New York, 1967).

[5]D. E. Weston, "Oblique Reflection of Inhomogeneous Acoustic Waves," J. Acoust. Soc. Am. **69**, 54–59 (1981).

[6]L. Sebbag, "Les Lois de la Réflexion-Réfraction des Ondes Evanescentes et les Ondes d'Interface," Ph.D. thesis, Université Paris VII (1987).

[7]O. Leroy, G. Quentin, and J. M. Claeys, "Energy Conservation for Inhomogeneous Plane Waves," J. Acoust. Soc. Am. **84**, 374–378 (1988).

[8]B. Poirée, "Les Ondes Planes Evanescentes dans les Fluides Parfaits et les Solides Elastiques," J. Acoustique **2**, 205–216 (1989).

[9]B. Poirée, "Complex Harmonic Plane Waves," in *Proceedings of the Symposium on Physical Acoustics: Fundamentals and Applications*, Kortrijk, Belgium, edited by O. Leroy and M. Breazeale (Plenum, New York, 1990), pp. 99–117.

[10]O. Leroy and K. Van Den Abeele, "Etude du comportement des ondes bornées, decomposées en ondes planes inhomogènes, dans l'approximité des angles critiques," *Acoustique Sous-Marine et Ultrasons* (L.M.A., Marseille, 1991), pp. 121–132.

[11]J. M. Claeys and O. Leroy, "Reflection and Transmission of Bounded Sound Beams on Half-spaces and through Plates," J. Acoust. Soc. Am. **72**, 585–590 (1982).

[12]M. Deschamps and C. L. Cheng, "Ondes Hétérogènes et Réflexion-Réfraction à l'Interface Liquide-non-Absorbant/Liquide-Thermovisqueux," Acustica **68**, 96–103 (1989).

[13]M. Deschamps and C. Changlin, "Réflexion-Réfraction de l'Onde Plane Hétérogène: Lois de Snell-Descartes et Continuité de l'Energie," J. Acoustique **2**, 229–240 (1989).

[14]M. Deschamps, "Réflexion-Réfraction de l'Onde Plane Hétérogène: Répartition de l'Energie," J. Acoustique **3**, 251–261 (1990).

[15]J. Roux, "Reflection and Refraction of Heterogeneous Waves at Plane Interfaces," in Ref. 9, pp. 155–164.

[16]B. Poirée and L. Sebbag, "Les Lois de la Réflexion-Réfraction des Ondes Planes Harmoniques Evanescentes. I. Mise en Equations," J. Acoustique **4**, 21–46 (1991).

[17]M. Deschamps, "L'Onde Plane Hétérogène et ses Applications en Acoustique Linéaire," J. Acoustique **4**, 269–305 (1991).

[18]L. M. Brekhovskikh, *Waves in Layered Media* (Academic, New York, 1960).

[19]T. J. Plona, M. Behravesh, and W. G. Mayer, "Rayleigh and Lamb Waves at Liquid-Solid Boundaries," Ultrasonics, 171–174 (July 1975).

[20]L. E. Pitts, T. J. Plona, and W. G. Mayer, "Theoretical Similarities of Rayleigh and Lamb Modes of Vibration," J. Acoust. Soc. Am. **60**, 374–377 (1976).

[21]T. J. Plona, L. E. Pitts, and W. G. Mayer, "Ultrasonic Bounded Beam Reflection and Transmission Effects at a Liquid/Solid Plate/Liquid Interface," J. Acoust. Soc. Am. **59**, 1324–1328 (1976).

[22]M. A. Breazeale, L. Adler, and L. Flax, "Reflection of a Gaussian Ultrasonic Beam from a Liquid-Solid Interface," J. Acoust. Soc. Am. **56**, 866–872 (1974).

[23]M. A. Breazeale, L. Adler, and J. H. Smith, "Energy redistribution of a Gaussian Ultrasonic Beam reflected from Liquid-Solid Interface," Sov. Phys. Acoust. **21**, 1–6 (1975).

[24]M. A. Breazeale, L. Adler, and G. W. Scott, "Interaction of Ultrasonic Waves Incident at the Rayleigh Angle onto a Liquid-Solid Interface," J. Appl. Phys. **48**, 530–536 (1977).

[25]T. D. K. Ngoc and W. G. Mayer, "Numerical Integration Method for Reflected Beam Profiles near Rayleigh Angle," J. Acoust. Soc. Am. **67**, 1149–1152 (1980).

[26]T. D. K. Ngoc and W. G. Mayer, "A General Description of Ultrasonic Nonspecular Reflection and Transmission Effects for Layered Media," IEEE Trans. Sonics Ultrason. **SU-27**(5), 229–236 (1980).

[27]O. Leroy and J. M. Claeys, "Optical Measurement of the Reflection Coefficient for Bounded Acoustic Waves," J. Acoust. Soc. Am. **75**, 1346–1351 (1984).

[28]O. Leroy and B. Poirée, "On the Reflection Coefficient of Acoustic Beams," Acustica **66**, 84–89 (1988).

[29]K. Van Den Abeele and O. Leroy, "Acoustooptic Reflection coefficient for Bounded Beams on Plates using Inhomogeneous Wave Description," in Ref. 9, pp. 647–655.

[30]G. Quentin, A. Derem, and B. Poirée, "The formalism of Evanescent Plane Waves and its Importance in the Study of the Generalized Rayleigh Wave," J. Acoustique **3**, 321–336 (1990).